Dominant Negative Mutants of Transducin-α That Block Activated Receptor†

Michael Natochin, Brandy Barren, and Nikolai O. Artemyev*

Department of Physiology and Biophysics, University of Iowa College of Medicine, Iowa City, Iowa 52242

Received February 24, 2006; Revised Manuscript Received April 3, 2006

ABSTRACT: Mutations counterpart to dominant negative RasSer17Asn in the α-subunits of heterotrimeric G-proteins are known to also produce dominant negative effects. The mechanism of these mutations remains poorly understood. Here, we examined the effects and mechanism of the Ser43Cys and Ser43Asn mutants of transducin-like chimeric Gtα* in the visual signaling system. Our analysis showed that both mutants have reduced affinity for GDP and are likely to exist in an empty—or partially occupied—pocket state. S43C and S43N retained the ability to interact with Gt$\beta\gamma$ and, as heterotrimeric proteins, bind to photoexcited rhodopsin (R*). The interaction with R* is unproductive as the mutants failed to bind GTPγS and become activated. S43C and S43N inhibited R*-dependent activation of Gtα* and Gtα, apparently by blocking R*. Finally, both Gtα* mutants lacked interaction with the γ-subunit of PDE6, an effector protein in phototransduction. These results indicate that the S43C and S43N mutants of Gtα* are dominant negative inhibitors that bind and block the activated receptor in a mechanism that parallels that of RasSer17Asn. Dominant negative mutants of Gtα sequestering R*, such as S43C and S43N, may become useful instruments in probing the mechanisms of visual dysfunctions caused by abnormal phototransduction signaling.

GTP-binding proteins transduce a vast number of signals inside a cell or across the cell membrane. Small monomeric and larger heterotrimeric proteins represent two distinct families in the superfamily of GTP-binding proteins. At the center of signaling by the two families is a conserved GTPase cycle that switches GTP-binding proteins between two principal states: inactive, GDP-bound, or activated, GTP-bound. A GTP-binding protein is activated by a guanine nucleotide exchange factor (GEF), which induces the release of bound GDP and its exchange for GTP. Intrinsic GTPase activity, often under the control of GTPase-activating proteins (GAPs), inactivates GTP-binding proteins. For heterotrimeric GTP-binding proteins (G-proteins), the function of GEFs is accomplished by agonist-activated G protein-coupled receptors (GPCRs), which induce GDP-release from Gα-subunits of cognate G-proteins, followed by binding of GTP and dissociation of GαGTP and G$\beta\gamma$ from the receptor (reviewed in refs *1*−*7*). Dominant negative mutants, particularly those of monomeric GTPases, have been very instrumental in delineating the complexity of signaling pathways by GTP-binding proteins. One of the best characterized dominant negative mutants is RasS17N (*6*, *8*). The serine residue, S17, binds the magnesium ion in the nucleotide-binding pocket of GDP- or GTP-bound Ras (*4*, *6*). The S17N mutation reduces Ras's affinity for both GDP and GTP and blocks its ability to reach an active conformation (*6*, *9*). While RasS17N fails to activate effector proteins, its nucleotide-free form binds tightly and sequesters Ras-GEFs, thereby inhibiting signaling by the wild-type Ras (*6*).

Mutations of the S17 counterpart residue in Gα subunits have been also shown to produce the dominant negative phenotype, but the mechanism of these mutants remains poorly understood (*10*−*13*). The Cys substitutions of Ser47 in Goα or Ser48 in Giα_2 yield dominant-negative mutants that seem to exert their effects through sequestration of G$\beta\gamma$ (*10*, *11*). A heterotrimer of Gα and G$\beta\gamma$ is a prerequisite for G-protein activation by a GPCR (*3*). Depletion of G$\beta\gamma$ by Gα mutants inhibits the activation of wild-type G-proteins and blocks G$\beta\gamma$-mediated pathways (*14*). However, the mechanism of dominant negative Gα mutants by G$\beta\gamma$-sequestration is nonselective and allows for the lingering presence of unblocked activated receptors. In contrast, the mechanism of the dominant negative S54N mutant of Gsα appears to be similar to that of RasS17N (*12*, *13*). The Gsα S54N mutant blocked the Gsα- and Gqα-mediated signaling from TSH receptor but not the Gqα-mediated signaling from the α_{1B}-adrenergic receptor, suggesting that GsαS54N blocks the TSH receptor (*13*). These findings indicate that the precise mechanism of the Ser mutants of Gα subunits may depend on the type of Gα or perhaps the nature of the substitution. Here, we examined the mechanism of the Ser mutations, S43C and S43N, introduced into the transducin-like chimeric protein Gtα*,[1] which is readily expressed in *Escherichia coli* (*15*). Transducin, a member of the Gi/Go family, mediates a classical phototransduction cascade in rod photoreceptor cells. The cascade is initiated by the interaction

† This work was supported by National Institutes of Health Grant EY12682.

* Author to whom correspondence should be addressed. Mailing address: Department of Physiology and Biophysics, University of Iowa College of Medicine, 5-532 Bowen Science Building, 51 Newton Rd., Iowa City, IA 52242. Tel: 319/335-7864. Fax: 319/335-7330. E-mail: nikolai-artemyev@uiowa.edu.

[1] Abbreviations: Gtα, rod G protein (transducin) α-subunit; Gtα*, effector-competent chimeric Gtα; PDE6, rod outer segment cGMP phosphodiesterase; Pγ, inhibitory subunit of PDE6; ROS (OS), rod outer segment(s); R*, light-activated rhodopsin; E-ROS, EDTA-stripped ROS membranes; GTPγS, guanosine 5′-O-(3-thiotriphosphate).

10.1021/bi060381e CCC: $33.50
Published on Web 04/29/2006

of photoexcited rhodopsin (R*) with transducin (Gt). GtαGTP is subsequently released to activate the effector enzyme PDE6 by displacing the inhibitory Pγ subunits from the catalytic core PDE6αβ. Hydrolysis of cGMP by activated PDE6 results in the closing of cGMP-gated channels in the photoreceptor plasma membrane (*16*). The ease of purification of rhodopsin in large quantities and the specificity of R*/transducin coupling makes this system an excellent model to probe the mechanism of dominant negative Gtα mutants. Furthermore, identification and characterization of dominant negative inhibitors of phototransduction may have important implications for potential therapies of specific forms of retinal degeneration caused by excessive visual signaling (*17*−*19*).

EXPERIMENTAL PROCEDURES

Materials. Guanosine 5′-[γ-^{35}S]thiotriphosphate triethylammonium salt (GTPγS; 1100 Ci/mmol), nicotinamide adenine [adenylate-^{32}P]dinucleotide (^{32}P-NAD; ∼1000 Ci/mmol), and PD-10 desalting columns were from Amersham Biosciences. GTP, GDP, and pertussis toxin were from Sigma-Aldrich. *Dpn*I restriction enzyme was from New England Biolabs, Inc. Turbo *Pfu* DNA polymerase was from Stratagene. DH5α and BL21(DE3) bacterial strains were from Invitrogen. His·Bind resin was from Novagen. Trypsin treated with L-(tosylamido-2-phenyl)-ethylchloromethylketone was from Worthington Biochemical Corp. Primers were synthesized by IDT, Inc. Bovine rod outer segment (ROS) membranes were prepared as described (*20*). EDTA-washed ROS (E-ROS) were prepared as described (*21*). Gt$\beta\gamma$ was purified as described (*22*).

*Mutagenesis and Expression of Gtα*S43C and Gtα*S43N.* The Gtα*S43C and Gtα*S43N mutants were obtained using the pHis6-Gtα* vector for expression of the transducin-like chimera, Gtα* (*15*), as a template in the PCR amplifications. Reverse Gtα* primer TCTGCTTGACAATGGT**ACA**CTTCCCGGATTCACCG and forward Gtα* primer CGGTGAATCCGGGAAG**TGT**ACCATTGTCAAGCAGA were used to obtain the mutation S43C (bold) by following the protocol of the QuikChange II site-directed mutageneis kit (Stratagene). Similarly, the reverse primer Gtα* TCTGCTTGACAATGGT**ATT**CTTCCCGGATTCACCG and forward Gtα* primer CGGTGAATCCGGGAAG**AAT**ACCATTGTCAAGCAGA were used to obtain the mutation S43N (bold). The constructs were sequenced at the University of Iowa DNA Core Facility. Gtα*, Gtα*S43C, and Gtα*S43N were expressed and purified as described (*23*).

Trypsin-Protection Assay. Gtα*, Gtα*S43C, and Gtα*S43N (2 μg) were incubated in 20 mM HEPES buffer (pH 8.0) containing 100 mM NaCl and 2 mM $MgSO_4$ (buffer A) and 50 μM GDP for 10 min at 25 °C. Where indicated, 10 mM NaF and 50 μM $AlCl_3$ were included in buffer A. For the GTPγS-bound Gtα*, Gtα*S43C, and Gtα*S43N, 2 μg of each protein was preincubated with bleached E-ROS (20 nM rhodopsin) and Gt$\beta\gamma$ (0.2 μg) in the presence of 50 μM GTPγS for 1 h at 25 °C. Where indicated, trypsin (10 μg/mL) was added and the digestion was carried out for 10 min at 25 °C. Digestions were stopped by heat treatment (100 °C) and the addition of SDS−PAGE sample buffer. Proteolytic fragments were analyzed by SDS−gel electrophoresis followed by Coomassie Blue staining.

Analysis of the Nucleotide-Bound State. Purified Gtα*, Gtα*S43C, and Gtα*S43N (400 μg) were passed through desalting PD-10 columns equilibrated with 20 mM Tris-HCl buffer (pH 8.0) containing 2 mM $MgSO_4$, and the proteins were denaturated by boiling for 10 min. The samples were centrifuged at 13000*g* for 10 min and then applied to YM-10 Microcon filters (Millipore). The guanine nucleotide composition of the filtrates was determined by chromatography on a MonoQ anion exchange column (Pharmacia) using a HPLC system (BioRad Model 2800). The column was equilibrated with 20 mM Tris-HCl buffer (pH 8.0) containing 5 mM $MgSO_4$ and 2 mM β-mercaptoethanol. Nucleotides eluted with a linear gradient of NaCl (0−800 mM/16 min) at the flow rate of 0.5 mL/min were monitored at 254 nm. Under these conditions, the elution times of the control GDP and GTP samples were 11.6 and 12.3 min, respectively.

Pertussis Toxin-Catalyzed ADP-Ribosylation. Gtα*, Gtα*S43C, and Gtα*S43N (0.5 μM) were mixed with Gt$\beta\gamma$ (0−3 μM) in buffer A. The reactions were initiated by the addition of 5 μM [^{32}P]NAD (0.3 μCi) and 3 μg/mL pertussis toxin (preactivated with 100 mM dithiothreitol and 0.25% SDS for 10 min at 30 °C) and allowed to proceed for 1 h at 25 °C. Aliquots from reaction mixtures were filtered through Whatman cellulose nitrate filters. The filters were washed three times with 20 mM Tris-HCl (pH 8.0) buffer containing 130 mM NaCl and 10 mM $MgSO_4$ and counted in a liquid scintillation counter. Additional aliquots from reaction mixtures were mixed with sample buffer for SDS−PAGE, heat-treated for 5 min at 100 °C, and analyzed by electrophoresis in 12% gels and autoradiography.

GTPγS Binding Assay. Gtα*, Gtα*S43C, and Gtα*S43N (1 μM) mixed with 2 μM Gt$\beta\gamma$ and E-ROS membranes (0.12 or 0.5 μM rhodopsin) were incubated for 2 min at 25 °C under room light conditions. Binding reactions were initiated with the addition of 20 μM [^{35}S]GTPγS (1 μCi). Aliquots of 20 μL were withdrawn at the indicated times, mixed with 1 mL of ice-cold 20 mM Tris-HCl (pH 8.0) buffer containing 130 mM NaCl, 2 mM $MgSO_4$, and 1 mM GTP, passed through Whatman cellulose nitrate filters (0.45 μm), and washed three times with 3 mL of the same buffer without GTP. The filters were dissolved in 5 mL of a xylene-based 3a70B counting cocktail (RPI Corp.), and [^{35}S]GTPγS was measured in a liquid scintillation counter. The initial rates for the binding reactions were calculated as the slopes of the linear fits.

To study the effects of the mutants on GTPγS binding to Gtα* and Gtα, indicated amounts of the mutants were preincubated with an equimolar concentration of Gt$\beta\gamma$ and indicated concentrations of E-ROS for 3 min at 25 °C, followed by the addition of Gtα*Gt$\beta\gamma$ or holotransducin, Gt (0.3 μM), and 20 μM [^{35}S]GTPγS (1 μCi). Time courses of GTPγS binding were determined at 25 °C (aliquots withdrawn at 1, 2, and 3 min), and the initial rates of the reactions were calculated and compared.

ROS Pull-Down Assay. E-ROS membranes were resuspended in 50 mM Tris-HCl (pH 7.4) buffer containing 100 mM NaCl and 5 mM $MgSO_4$. The rhodopsin concentration was calculated using the extinction coefficient 40 600 M^{-1} cm^{-1} at A_{500} (*24*). Gtα*, Gtα*S43C, and Gtα*S43N (2μM) were mixed with E-ROS (0.5 μM rhodopsin) in the absence or presence of Gt$\beta\gamma$ (2 μM) and incubated for 20 min at 25 °C under room light conditions in 50 mM Tris-HCl (pH 7.4) buffer containing 100 mM NaCl and 5 mM $MgSO_4$. The

samples were centrifuged at 15000*g* for 15 min at 4 °C. Pellets were resuspended in the same buffer and centrifuged three more times. The pellets were resuspended in 20 mM Tris-HCl (pH 7.4) buffer containing 5 mM $MgSO_4$, and one-half of the membrane suspension (20 μL) was added to SDS sample buffer, followed by heat treatment (100 °C, 5 min). The other half was incubated for 30 min at 25 °C in a volume of 300 μL of the same buffer containing 3 mM GTPγS. The samples were centrifuged at 15000*g* for 15 min at 4 °C. The supernatants were collected and concentrated using Speed Vac (Savant), and SDS sample buffer was added to the concentrated supernatants, followed by heat treatment (100 °C, 5 min). The pellets were resuspended in the GTPγS-containing buffer, incubated for 30 min at 25 °C, and centrifuged at 15000*g* for 15 min at 4 °C. This step was repeated twice. Finally, SDS sample buffer was added to the pellets followed by heat treatment (100 °C, 5 min). Samples were analyzed by SDS−gel electrophoresis followed by Coomassie Blue staining.

"Extra" Metarhodopsin II Assay. The absorbance spectra of E-ROS (4 μM rhodopsin) were measured at 4 °C in the absence and presence of 2 μM transducin or 5 μM Gtα*, Gtα*S43C, or Gtα*S43N prebound with equimolar concentrations of Gt$\beta\gamma$. The assay buffer contained 10 mM MOPS (pH 7.6), 2 mM $MgSO_4$, 1 mM dithiotreitol, 200 mM NaCl, and, where indicated, 100 μM GTPγS. A dark spectrum was recorded first. A second spectrum was measured 1 min after 10 s of bleaching with a 150 W light source at a distance of 10 cm. The difference between the two spectra was calculated. Metarhodopsin II was assessed as the difference between the absorbance at 380 and 420 nm (*21*, *25*).

Pγ Fluorescence-Binding Assay. Fluorescence-binding measurements were performed on a F-2500 fluorescence spectrophotometer (Hitachi) in 0.5 mL of buffer A at 25 °C. Fluorescence of Pγ labeled with 3-(bromoacetyl)-7-diethylaminocoumarin (PγBC, 15 nM) (*26*) was measured with an excitation of 445 nm and emission of 495 nm in the presence of increasing concentrations of the GDP-, AlF_4^--, or GTPγS-bound Gtα*, Gtα*S43C, or Gtα*S43N. The AlF_4^-- and GTPγS-bound proteins were obtained by preincubation of 10 mM NaF and 50 μM $AlCl_3$ for 10 min, or 50 μM GTPγS in the presence of bleached uROS membranes (100 nM rhodopsin) and Gt$\beta\gamma$ (100 nM) for 1 h, followed by centrifugation for 15 min at 13000*g*.

Miscellaneous Procedures. Protein concentrations were measured using IgG as a standard as described (*27*). SDS−PAGE was performed using 12% acrylamide gels. GraphPad Prizm (version 4) was used to fit the experimental data and plot the graphs. Results are expressed as mean ± SE for three independent experiments.

RESULTS

*Expression and Trypsin Sensitivity of the Gtα*S43C and Gtα*S43N Mutants.* Two mutations, S43C and S43N, were introduced into the Gtα-like chimeric protein Gtα*, which is readily expressed in *E. coli* (*15*). This effector competent Gtα* was generated previously, based on the Gtα/Giα Chi8 (*23*), by introducing two Gtα-specific residues H244 and N247 (*15*). The yields of purified Gtα*S43C and Gtα*S43N mutants were similar (~1 mg/L of culture). A trypsin protection assay was performed to assess the folding and

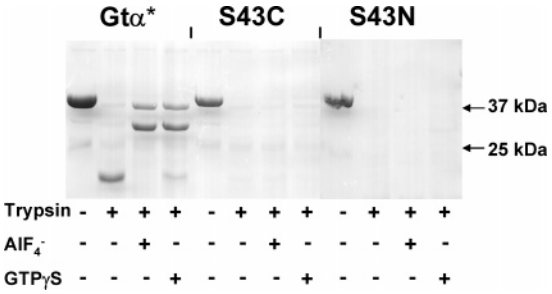

FIGURE 1: Trypsin-protection assay of Gtα*, Gtα*S43C, and Gtα*S43N. Gtα*, Gtα*S43C, and Gtα*S43N (2 μg) were treated with trypsin (10 μg/mL) for 10 min at 25 °C in the presence of 50 μM GDP alone, or 50 μM GDP, 10 mM NaF, and 50 μM $AlCl_3$. The GTPγS-bound proteins were obtained as described under Experimental Procedures. Samples were analyzed by SDS−PAGE in 12% gels and stained with Coomassie Blue.

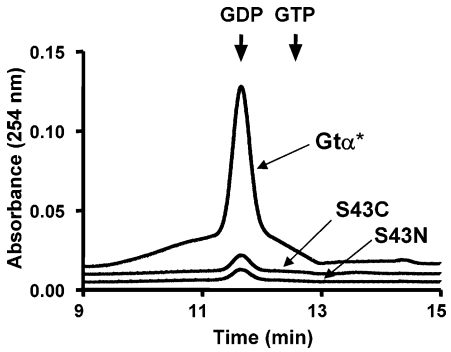

FIGURE 2: Analysis of the nucleotides released from Gtα*, Gtα*S43C, and Gtα*S43N. Nucleotides bound to Gtα*, Gtα*S43C, and Gtα*S43N (400 μg) were released by boiling for 10 min, filtrated through YM-10 Microcon filters, and separated on a MonoQ column as described under Experimental Procedures. The retention times for the GDP and GTP standards were 11.6 and 12.3 min, respectively.

nucleotide-binding state of the mutants. When Gtα* becomes activated (GDP-AlF_4^-- or GTPγS-bound), a conformational change occurs which protects the switch II region from tryptic cleavage and results in the appearance of a ~34 kDa band. As expected, the trypsin-protection test of Gtα* showed a ~20 kDa band in the GDP-bound state, and a ~34 band for the AlF_4^-- and GTPγS-activated conformations (Figure 1). In contrast, the Gtα*S43C and Gtα*S43N mutants were fully proteolyzed by trypsin regardless of the presence of GDP, GDP-AlF_4^-, or GTPγS (Figure 1). The absence of the ~20 and ~34 kDa bands indicates that either the mutants are deficient in GDP and GTP binding or their guanine nucleotide-bound conformations are different from those of Gtα*.

*Nucleotide Bound State of Gtα*S43C and Gtα*S43N.* To further elucidate the nucleotide-bound state of Gtα*S43C and Gtα*S43N, the mutants were denaturated to release bound nucleotide, which was identified by HPLC. The HPLC profiles show that the Gtα*S43C and Gtα*S43N mutants contain a negligible amount of bound GDP compared to Gtα* when the same amount of proteins was analyzed (Figure 2). This correlates with the results of the trypsin-protection test and shows that the mutants have a severely reduced affinity for GDP and are likely to exist in an empty-pocket state.

Gt$\beta\gamma$-Dependent Pertussis Toxin-Catalyzed ADP-Ribosylation of Gtα, Gtα*S43C, and Gtα*S43N.* We next exam-

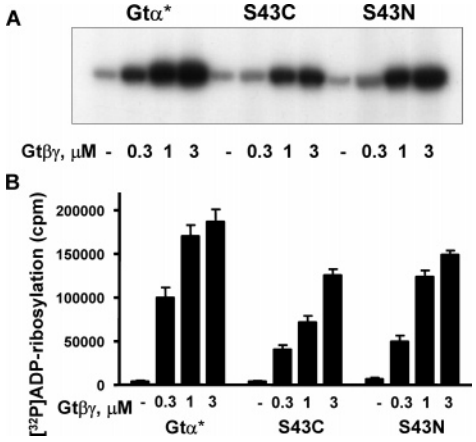

FIGURE 3: Gt$\beta\gamma$-dependent ADP-ribosylation of Gtα*, Gtα*S43C, and Gtα*S43N. Pertussis toxin catalyzed [^{32}P]ADP-ribosylation of Gtα*, Gtα*S43C, and Gtα*S43N (0.5 μM each) was performed in the presence of increasing concentrations of Gt$\beta\gamma$ (0, 0.3, 1.0, and 3 μM) as described under Experimental Procedures. Samples were analyzed by SDS−PAGE in 12% gels followed by autoradiography (A) or by filtering through Whatman cellulose nitrate filters and counting the filters in a liquid scintillation counter (B).

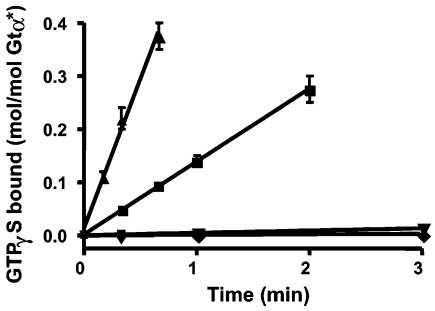

FIGURE 4: Kinetics of GTPγS binding to Gtα*, Gtα*S43C, and Gtα*S43N. The binding of GTPγS to Gtα* (■, ▲), Gtα*S43C (▼), and Gtα*S43N (◆; 1 μM each) in the presence of 2 μM Gt$\beta\gamma$ and E-ROS membranes (120 nM rhodopsin ■; 500 nM rhodopsin ▲, ▼, ◆) was initiated by the addition of 20 μM [^{35}S]GTPγS. Aliquots were withdrawn at the indicated time points, passed through Whatman cellulose nitrate filters (0.45 μm), and counted in a liquid scintillation counter. The k_{app} values (min^{-1}) are (■) 0.14 ± 0.01 and (▲) 0.56 ± 0.04.

ined the ability of the mutants to interact with Gt$\beta\gamma$. Gtα*GDP is known to be ADP-ribosylated by pertussis toxin at Cys347 (*28*, *29*). Since holotransducin Gt$\alpha\beta\gamma$ is a notably better substrate than the Gtα-subunit alone (*30*), ADP-ribosylation by pertussis toxin is a sensitive assay to assess the interaction between Gtα and Gt$\beta\gamma$. Gtα*, Gtα*S43C, and Gtα*S43N all showed increased ADP-ribosylation in a Gt$\beta\gamma$ dose-dependent manner (Figure 3). Although the Gtα*S43C and Gtα*S43N mutants required slightly higher concentrations of Gt$\beta\gamma$ to produce equivalent effects compared to Gtα*, they are clearly capable of interacting with Gt$\beta\gamma$.

*Gtα*S43C and Gtα*S43N Are Not Activated by R**. The ability of Gtα*S43C and Gtα*S43N to interact with Gt$\beta\gamma$ allowed us to test the functional coupling of the heterotrimeric mutants to R*. Control experiments demonstrated the R*-dependent kinetics of GTPγS binding to Gtα* in the presence of Gt$\beta\gamma$ (Figure 4). Unlike Gtα*, both Gtα*S43C and Gtα*S43N did not appreciably bind GTPγS even when using a relatively high concentration of R* (Figure 4). This result suggests that either the mutants either fail to interact

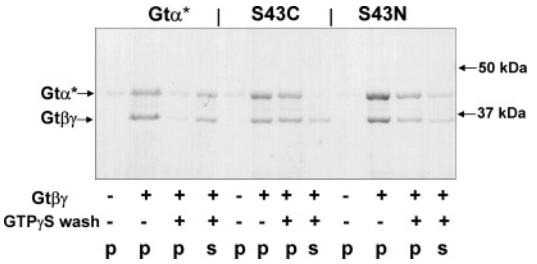

FIGURE 5: Binding of Gtα*, Gtα*S43C, and Gtα*S43N to ROS membranes. Gtα*, Gtα*S43C, and Gtα*S43N (2 μM each) and EDTA-stripped ROS membranes containing 0.5 μM rhodopsin were incubated in the absence or presence of Gt$\beta\gamma$ (2 μM) for 20 min at 25 °C, centrifuged, and washed twice with isotonic buffer. Aliquots of E-ROS were analyzed by SDS−electrophoresis (left two lanes for each construct), while additional aliquots of E-ROS with bound Gtα*$\beta\gamma$ or mutants were used for extraction with hypotonic buffer containing 3 mM GTPγS as described under Experimental Procedures. The membrane pellets (p) and the supernatants (s) after the addition of GTPγS were analyzed by SDS−electrophoresis (right two lanes for each construct).

with R* or they bind to R*, but fail to subsequently bind GTPγS and assume an activated conformation.

Binding of Gtα, Gtα*S43C, and Gtα*S43N to R**. To determine if Gtα*S43C and Gtα*S43N retained the ability to bind to R*, direct mutant binding to E-ROS was investigated in the presence or absence of Gt$\beta\gamma$ (Figure 5). Both mutants bound to E-ROS membranes in the presence, but not in the absence, of Gt$\beta\gamma$. Moreover, the mutant binding was comparable to the binding of Gtα*. The addition of GTPγS to the E-ROS membranes caused activation and elution of Gtα*, but not Gtα*S43C, supporting the mutant's inability to bind guanine nucleotides (Figure 5). The GTPγS-induced elution of Gtα*S43N was markedly reduced with most of the mutant remaining membrane-bound (Figure 5).

To prove that the binding of Gtα*S43C and Gtα*S43N to E-ROS membranes reflects their interaction with R*, we performed the MII-stabilization assay (*25*). Through a chain of intermediate photoproducts, photoexcitation of rhodopsin leads to an equilibrium between metarhodopsin I and metarhodopsin II (MII) (*31*), of which MII (R*) is the photoproduct that binds and activates Gt (*32*). When ROS membranes are bleached in the presence of Gt, the stable interaction between MII and Gt in the absence of GTP leads to the formation of extra MII (*25*). The spectroscopic measurements of MII showed that both Gtα*S43C and Gtα*S43N stabilize MII similar to native Gtα and Gtα* (Figure 6). As expected, the addition of GTPγS reversed the MII stabilization effects of Gtα and Gtα*. In contrast, GTPγS had little or no effect on the MII formation in the presence of Gtα*S43C and Gtα*S43N (Figure 6).

*Gtα*S43C and Gtα*S43N Inhibit R*-Stimulated GTPγS Binding to Gtα*and Gtα.* Intact binding of Gtα*S43C and Gtα*S43N to R* coupled with their inability to bind GTPγS and be released from the complex with receptor indicated that the mutants may compete with Gtα* for R* and block Gtα* activation. To test this hypothesis, we examined GTPγS binding to Gtα* in the presence of increasing concentrations of the mutants. Gtα* and the mutants were reconstituted with equimolar amounts of Gt$\beta\gamma$ to exclude effects due to Gt$\beta\gamma$ sequestration. As shown in Figure 7A, the initial rates of GTPγS binding to Gtα* decreased in a Gtα*S43C and Gtα*S43N dose-dependent manner. Gtα*S43N

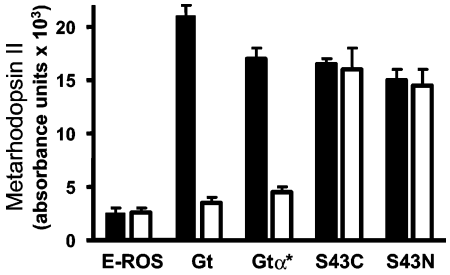

FIGURE 6: The meta II stabilization by Gtα*, Gtα*S43C, and Gtα*S43N. The absorbance spectra of E-ROS (4 μM rhodopsin) were measured at 4 °C in the absence and presence of 2 μM holotransducin (Gt) or 5 μM Gtα*, Gtα*S43C, or Gtα*S43N prebound with equimolar Gt$\beta\gamma$. The assay buffer contained 10 mM MOPS (pH 7.6), 2 mM $MgSO_4$, 1 mM dithiotreitol, and 200 mM NaCl (filled bars), and 100 μM GTPγS (open bars). A dark spectrum was recorded first. A second spectrum was measured 1 min after 10 s of bleaching with a 150 W light source at a distance of 10 cm. The difference between the two spectra was calculated. Metarhodopsin II was assessed as the difference between the absorbance at 380 and 420 nm.

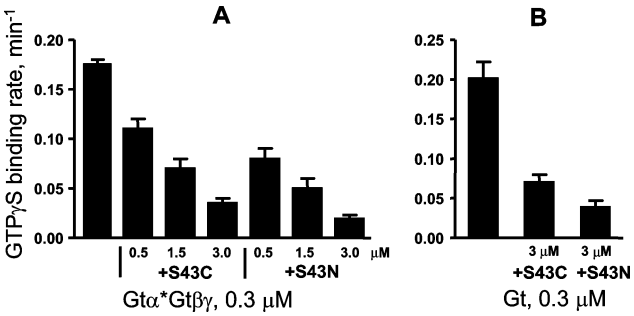

FIGURE 7: Gtα*S43C and Gtα*S43N inhibit R*-stimulated GTPγS binding to Gtα* and Gtα. Gtα*S43C and Gtα*S43N (0.5−3 μM) were preincubated with an equimolar concentration of Gt$\beta\gamma$ and E-ROS (A, 150 nM, B, 30 nM rhodopsin) for 3 min at 25 °C, followed by the addition of Gtα*Gt$\beta\gamma$ (A) or holotransducin, Gt (B) (0.3 μM each), and 20 μM [^{35}S]GTPγS (1 μCi). Time courses of GTPγS binding were determined at 25 °C (aliquots withdrawn at 1, 2, and 3 min), and the initial rates of the reactions were calculated.

appeared to be a somewhat more potent inhibitor compared to Gtα*S43C. The addition of a 10-fold excess of Gtα*S43N over Gtα* reduced the GTPγS binding rate by ~90% (Figure 7A). We also examined the ability of Gtα*S43C and Gtα*S43N to block the R*-dependent activation of native Gt isolated from bovine ROS. In this experiment, a lower concentration of E-ROS (30 nM rhodopsin) was used to achieve an initial GTPγS binding rate similar to that for Gtα*Gt$\beta\gamma$ using 150 nM rhodopsin. The mutants also markedly inhibited GTPγS binding to Gt (Figure 7B).

*Gtα*S43C and Gtα*S43N Fail To Interact with the γ-Subunit of PDE6.* GDP-bound Gtα is known to have a basal affinity for the PDE6 γ-subunit, which is markedly enhanced in the AlF_4^-- or GTPγS-activated conformations of Gtα (*26*, *33*). This increase in the interaction with Pγ can be monitored by a binding assay utilizing fluorescently labeled Pγ, PγBC (*26*). The fluorescence binding assay was performed to determine whether the conformations of Gtα*S43C and Gtα*S43N allow them to bind Pγ. No interaction of either mutant with PγBC was detected, regardless of the presence of GDP, GDP-AlF_4^- (Figure 8), or GTPγS (not shown). In control experiments, Gtα* displayed an ~8-fold and a ~14-fold increase in the affinity

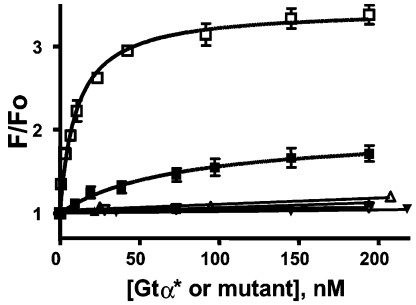

FIGURE 8: Binding of Gtα*, Gtα*S43C, and Gtα*S43N to PγBC. The relative increase in fluorescence (F/Fo) of PγBC (15 nM) (excitation at 445 nm, emission at 495 nm) was determined in the presence of increasing concentrations of Gtα* (■, □), Gtα*S43C (▲, △), and Gtα*S43N (▼, ▽) in the GDP- (closed symbols) or GDP-AlF_4^--bound (open symbols) conformations. The K_d values for Gtα* (nM) are (■) 75 ± 8 and (□) 9 ± 2.

for PγBC when activated by AlF_4^- (Figure 8) and GTPγS, respectively (not shown).

DISCUSSION

A number of mutant Gα subunits exerting often only weak dominant negative effects have been described (*34*−*37*). Activation of heterotrimeric G-proteins by agonist-bound GPCRs releases potentially two signaling species: GαGTP and G$\beta\gamma$. Consequently, dominant negative mutants of Gα might act by blocking GPCRs, by inhibiting GαGTP-mediated activation of effectors or by sequestering G$\beta\gamma$. To date, no dominant negative mutant Gα subunits that effectively prevent activation of effectors by GαGTP have been identified. Two mutations of Gsα, G225T and G226A, were shown to reduce its ability to bind GTP and assume an activated conformation (*34*, *35*). These Gsα mutants were reported to inhibit hormone-induced stimulation of adenylyl cyclase. Corresponding mutations in $Gi\alpha_2$ also produced dominant negative effects (*36*, *37*). The main mechanism of the Gα mutants with the impaired ability to undergo activational conformational change is likely based on the sequestration of G$\beta\gamma$ (*14*). Gα mutants sequestering only G$\beta\gamma$ would be potent inhibitors of G-protein signaling mediated by G$\beta\gamma$. However, such mutants would not be efficient in blocking G-protein pathways with GαGTP as transducers due to the catalytic role of G$\beta\gamma$ during G-protein activation by GPCRs (*14*). Concentrations of G$\beta\gamma$ much lower than stoichiometric may allow significant activation of Gα. Therefore, the most effective and specific mechanism for a dominant negative Gα should involve the sequestration of activated GPCRs, just as RasS17N binds and blocks RasGEFs. A stable empty-pocket complex between G$\alpha\beta\gamma$ and GPCR is formed in the absence of guanine nucleotides (*3*, *5*). With this rationale, a triple dominant negative mutant that combined mutations reducing Gsα's affinity for both GDP and GTP was designed (*14*). This mutant was shown to be a robust and selective inhibitor of Gs-dependent hormonal stimulation of adenylyl cyclase, presumably through the sequestration of activated GPCR (*14*). Still, mutants in Gα subunits with a substitution at the position corresponding to RasS17 remain the best candidates as singly mutated dominant negative inhibitors. The mechanism of these mutants remains controversial (*10*−*13*). GsαS54N was shown to block the TSH receptor (*13*), whereas GoαS47C and $Gi\alpha_2$S48C were reported to act through sequestration of G$\beta\gamma$ (*10*, *11*).

We have generated the S43C and S43N mutants of transducin-like Gtα* and examined their effects on the rhodopsin/transducin/PDE6 visual signaling pathway. Our results demonstrate that both mutants have reduced affinity for guanine nucleotides and are likely to exist in an empty or partially occupied pocket state. Gtα*S43C and Gtα*S43N retained the ability to interact with G$\beta\gamma$ and, as heterotrimeric proteins, bind R*. The interaction with R* is unproductive in that the mutants fail to bind GTPγS and become activated. Moreover, by binding and blocking R*, Gtα*S43C and Gtα*S43N can inhibit R*-dependent activation of Gtα. Finally, Gtα*S43C and Gtα*S43N did not show any interaction with the effector protein. Therefore, both mutants are dominant negative inhibitors that bind and block the activated receptor similarly to the effects of GsαS54N (*13*). Yet, unlike the Gtα* mutants, GsαS54N appears to retain some GTP-binding capacity and can increase basal cellular cAMP levels in the absence of hormonal stimulation (*12*, *13*).

Our results suggest that the dominant negative mechanism of the Ser residue mutations in Gα subunits is not dependent on the type of G-protein (Gs or Gi/o/t) or on the type of mutation (Asn or Cys). Theoretically, the Ser to Asn or Cys mutants in all Gα families should be capable to some extent of blocking activated cognate GPCRs. This study is the second report of a dominant negative transducin-α. A recent study had reported a dominant negative phenotype for transducin-α mutant R238E (*38*). However, our subsequent investigation of Gtα*R238E revealed properties entirely inconsistent with those of a dominant negative inhibitor (*39*). In contrast to the reported phenotype (*38*), we found that Gtα*R238E binds GDP and GTP, and is fully capable of activational coupling to R* (*39*).

A number of visual disorders, including certain forms of inherited and light-induced retinal degenerations or stationary night blindness, are caused by excessive phototransduction signaling (*17*−*19*). Often, the source of excessive signaling is constitutive activity or inadequate inactivation of the visual receptor (*17*−*19*). Dominant negative mutants of Gtα that sequester R* and block activation of native Gt, such as S43C and S43N, may become very useful instruments in probing the mechanisms of visual dysfunctions. They could also potentially serve as therapeutical tools for more severe forms of retinal degeneration due to abnormal phototransduction.

REFERENCES

1. Gilman, A. G. (1987) G proteins: transducers of receptor-generated signals, *Annu. Rev. Biochem. 56*, 615−649.
2. Lowy, D. R., and Willumsen, B. M. (1993) Function and regulation of ras, *Annu. Rev. Biochem. 62*, 851−891.
3. Bourne, H. R. (1997) How receptors talk to trimeric G proteins, *Curr. Opin. Cell Biol. 9*, 134−142.
4. Geyer, M., and Wittinghofer, A. (1997) GEFs, GAPs, GDIs and effectors: taking a closer (3D) look at the regulation of Ras-related GTP-binding proteins, *Curr. Opin. Struct. Biol. 7*, 786−792.
5. Hamm, H. E. (1998) The many faces of G protein signaling, *J. Biol. Chem. 273*, 669−672.
6. Feig, L. A. Tools of the trade: use of dominant-inhibitory mutants of Ras-family GTPases (1999) *Nat. Cell Biol. 1*, E25−E27.
7. Pierce, K. L., Premont, R. T., and Lefkowitz, R. J. (2002) Seven-transmembrane receptors. *Nat. Rev. Mol. Cell Biol. 3*, 639−650.
8. Powers, S., O'Neill, K., and Wigler, M. (1989) Dominant yeast and mammalian RAS mutants that interfere with the CDC25-dependent activation of wild-type RAS in Saccharomyces cerevisiae, *Mol. Cell. Biol. 9*, 390−395.
9. John, J., Rensland, H., Schlichting, I., Vetter, I., Borasio, G. D., Goody, R. S., and Wittinghofer, A. (1993) Kinetic and structural analysis of the Mg^{2+}-binding site of the guanine nucleotide-binding protein p21H-ras, *J. Biol. Chem. 268*, 923−929.
10. Slepak, V. Z., Quick, M. W., Aragay, A. M., Davidson, N., Lester, H. A., and Simon, M. I. (1993) Random mutagenesis of G protein α subunit G(o)α. Mutations altering nucleotide binding, *J. Biol. Chem. 268*, 21889−21894.
11. Slepak, V. Z., Katz, A., and Simon, M. I.(1995) Functional analysis of a dominant negative mutant of Gαi2, *J. Biol. Chem. 270*, 4037−4041.
12. Cleator, J. H., Mehta, N. D, Kurtz, D. T., and Hildebrandt, J. D. (1999) The N54 mutant of Gαs has a conditional dominant negative phenotype which suppresses hormone-stimulated but not basal cAMP levels, *FEBS Lett. 443*, 205−208.
13. Cleator, J. H., Ravenell, R., Kurtz, D. T., and Hildebrandt JD. (2004) A dominant negative Gαs mutant that prevents thyroid-stimulating hormone receptor activation of cAMP production and inositol 1,4,5-trisphosphate turnover: competition by different G proteins for activation by a common receptor, *J. Biol. Chem. 279*, 36601−36607.
14. Iiri, T., Bell, S. M., Baranski, T. J., Fujita, T., and Bourne, H. R. (1999) Gsα mutant designed to inhibit receptor signaling through Gs, *Proc. Natl. Acad. Sci. U.S.A.* 96, 499−504.
15. Muradov, K. G., and Artemyev, N. O. (2000) Loss of the effector function in a transducin-α mutant associated with Nougaret night blindness, *J. Biol. Chem. 275*, 6969−6974.
16. Arshavsky, V. Y, Lamb, T. D., and Pugh, E. N., Jr. (2002) G proteins and phototransduction, *Annu. Rev. Physiol. 264*, 153−187.
17. Dryja, T. P. (2000) Molecular genetics of Oguchi disease, fundus albipunctatus, and other forms of stationary night blindness: LVII Edward Jackson Memorial Lecture, *Am. J. Ophthalmol. 130*, 547−563.
18. Pierce, E. A. (2001) Pathways to photoreceptor cell death in inherited retinal degenerations, *Bioessays 23*, 605−618.
19. Lem, J., and Fain, G. L. (2004) Constitutive opsin signaling: night blindness or retinal degeneration?, *Trends Mol. Med. 10*, 150−157.
20. Papermaster, D. S., and Dreyer, W. J. (1974) Rhodopsin content in the outer segment membranes of bovine and frog retinal rods, *Biochemistry 13*, 2438−2444.
21. Dratz, E. A., Furstenau, J. E., Lambert, C. G., Thireault, D. L., Rarick, H., Schepers, T., Pakhlevaniants, S., and Hamm, H. E. (1993) NMR structure of a receptor-bound G-protein peptide, *Nature 363*, 276−281.
22. Kleuss, C., Pallast, M., Brendel, S., Rosenthal, W., and Schultz, G. (1987) Resolution of transducin subunits by chromatography on blue sepharose, *J. Chromatogr. 407*, 281−289.
23. Skiba, N. P., Bae, H., and Hamm, H. E. (1996) Mapping the effector binding sites of transducin α-subunit using Gαt/Gαi1 chimeras, *J. Biol. Chem. 271*, 413−424.
24. Wald, G., and Brown, P. K. (1953) The molar extinction of rhodopsin, *J. Gen. Physiol. 37*, 189−200.
25. Emeis, D., Kuhn, H., Reichert, J., and Hofmann, K. P. (1982) Complex formation between metarhodopsin II and GTP-binding protein in bovine photoreceptor membranes leads to a shift of the photoproduct equilibrium, *FEBS Lett. 143*, 29−34.
26. Artemyev, N. O. (1997) Binding of transducin to light-activated rhodopsin prevents transducin interaction with the rod cGMP phosphodiesterase γ-subunit, *Biochemistry 36*, 4188−4193.
27. Bradford, M. M. (1976) A rapid and sensitive method for the quantitation of microgram quantities of proteins utilizing the principle of protein-dye binding, *Anal. Biochem. 72*, 248−254.
28. van Dop, C., Yamanaka, G., Steinberg, F., Sekura, R. D., Manclark, C. R., Stryer, L., and Bourne, H. R. (1984) ADP-ribosylation of transducin by pertussis toxin blocks the light-stimulated hydrolysis of GTP and cGMP in retinal photoreceptors, *J. Biol. Chem. 259*, 23−26.
29. West, R. E., Jr., Moss, J., Vaughan, M., Liu, T., and Liu, T. Y. (1985) Pertussis toxin-catalyzed ADP-ribosylation of transducin. Cysteine 347 is the ADP-ribose acceptor site, *J. Biol. Chem. 260*, 14428−14430.
30. Watkins, P. A., Burns, D. L., Kanaho, Y., Liu, T. Y., Hewlett, E. L., and Moss, J. (1985) ADP-ribosylation of transducin by pertussis toxin, *J. Biol. Chem. 260*, 13478−13482.
31. Wald, G. (1968) The molecular basis of visual excitation, *Nature 219*, 800−807.

32. Bennett, N, Michel-Villaz, M., and Kuhn, H. (1982) Light-induced interaction between rhodopsin and the GTP-binding protein. Metarhodopsin II is the major photoproduct involved, *Eur. J. Biochem. 127*, 97−103.
33. Otto-Bruc, A., Antonny, B., Vuong, T. M., Chardin, P., and Chabre, M. (1993) Interaction between the retinal cyclic GMP phosphodiesterase inhibitor and transducin. Kinetics and affinity studies, *Biochemistry 32*, 8636−8645.
34. Miller, R. T., Masters, S. B., Sullivan, K. A., Beiderman, B., and Bourne, H. R. (1988) A mutation that prevents GTP-dependent activation of the α chain of Gs, *Nature 334*, 712−715.
35. Osawa, S., and Johnson, G. L. (1991) A dominant negative Gαs mutant is rescued by secondary mutation of the α chain amino terminus, *J. Biol. Chem. 266*, 4673−4676.
36. Hermouet, S., Merendino, J. J., Jr., Gutkind, J. S., and Spiegel, A. M. (1991) Activating and inactivating mutations of the alpha subunit of Gi2 protein have opposite effects on proliferation of NIH 3T3 cells, *Proc. Natl. Acad. Sci. U.S.A.* 88, 10455−10459.
37. Murray-Whelan, R., Reid, J. D., Piuz, I., Hezareh, M., and Schlegel, W. (1995) The guanine-nucleotide-binding protein subunit Gαi2 is involved in calcium activation of phospholipase A2. Effects of the dominant negative Gαi2 mutant, [G203T]Gαi2, on activation of phospholipase A2 in Chinese hamster ovary cells, *Eur. J. Biochem. 230*, 164−169.
38. Pereira, R., and Cerione, R. A. (2005) A switch 3 point mutation in the α subunit of transducin yields a unique dominant-negative inhibitor. *J. Biol. Chem. 280*, 35696−35703.
39. Barren, B., Natochin, M., and Artemyev, N. O. (2006) Mutation R238→E in transducin-α yields a GTPase and effector-deficient, but not dominant-negative G-protein α-subunit, *Mol. Vis.*, in press.

BI060381E